Inorg. Chem. **2007**, *46*, 2193–2203

Distinct Mechanisms of Bridging-Oxo Exchange in Di-μ-O Dimanganese Complexes with and without Water-Binding Sites: Implications for Water Binding in the O_2-Evolving Complex of Photosystem II

Ranitendranath Tagore, Robert H. Crabtree, and Gary W. Brudvig*

Department of Chemistry, Yale University, P.O. Box 208107, New Haven, Connecticut 06520-8107

Received October 13, 2006

Isotopic exchange between oxygens of water and μ-O bridges in the di-μ-O dimanganese complexes, $[(\text{mes–terpy})_2Mn_2^{III/IV}(\mu\text{-O})_2(H_2O)_2](NO_3)_3$ (**1**, mes–terpy = 4′-mesityl-2,2′:6′,2″-terpyridine) and $[(\text{phen})_4Mn_2^{III/IV}(\mu\text{-O})_2](ClO_4)_3$ (**2**, phen = 1,10-phenanthroline), has been investigated by a study of the kinetics of exchange. The data provide evidence for distinct mechanisms of exchange in **1** and **2** and suggest that these differences arise due to the presence and absence of terminal water-binding sites in **1** and **2**, respectively. Exchange of oxygen atoms between water and μ-O bridges must involve the elementary steps of bridge protonation, deprotonation, opening, and closing. On the basis of the existing literature on these reactions in oxo-bridged metal complexes and our present data, we propose pathways of exchange in **1** and **2**. The mechanism proposed for **1** involves an initial fast protonation of an oxo-bridge by water coordinated to Mn^{IV}, followed by a slow opening of the protonated bridge as proposed earlier for an analogous complex on the basis of DFT calculations. The mechanism proposed for **2** involves initial dissociation of phen, followed by coordination of water at the vacated sites, as observed for rearrangement of **2** to a trinuclear complex. The subsequent steps are proposed to be analogous to those for **1**. Our results are discussed in the context of data on ^{18}O-labeled water isotope exchange in photosystem II and provide support for the existence of fully protonated terminal waters bound to Mn in the O_2-evolving complex of photosystem II.

Introduction

Photosystem II (PSII), the membrane protein complex catalyzing the light-driven oxidation of water into molecular oxygen, contains manganese as an essential cofactor.[1,2] Extended X-ray absorption fine structure (EXAFS) spectroscopy of PSII has provided general consensus that the manganese atoms in PSII form a structure consisting of $Mn_2(\mu\text{-O})_2$ units.[3] Recent crystallographic studies are consistent with this notion,[4−8] with Ferreira et al. modeling the oxygen-evolving complex (OEC) of PSII as a cuboidal $Mn_3Ca(\mu\text{-O})_4$ cluster connected to a fourth Mn via a μ-O bridge.[6]

Proposed molecular mechanisms of water oxidation by the OEC need to specify the timing and nature of substrate (water) binding by the catalytic center. The timing of water binding is specified by the S-states (S_0 through S_4) of the OEC at which substrate waters bind. The nature of binding is specified by the site and mode of binding; for example, terminal aqua or hydroxo ligands bound to a single Mn or Ca atom[9−14] or μ-oxo or μ-hydroxo bridges between multiple metal centers.[3,15−22] Important constraints have been provided

* To whom correspondence should be addressed. E-mail: gary.brudvig@yale.edu.

(1) McEvoy, J. P.; Brudvig, G. W. *Chem. Rev.* **2006**, *106*, 4455−4483.
(2) Debus, R. J. *Biochim. Biophys. Acta* **1992**, *1102*, 269−352.
(3) Robblee, J. H.; Cinco, R. M.; Yachandra, V. K. *Biochim. Biophys. Acta* **2001**, *1503*, 7−23.
(4) Zouni, A.; Witt, H.-T.; Kern, J.; Fromme, P.; Krauss, N.; Saenger, W.; Orth, P. *Nature (London)* **2001**, *409*, 739−743.
(5) Kamiya, N.; Shen, J.-R. *Proc. Natl. Acad. Sci. U.S.A.* **2003**, *100*, 98−103.
(6) Ferreira, K. N.; Iverson, T. M.; Maghlaoui, K.; Barber, J.; Iwata, S. *Science* **2004**, *303*, 1831−1838.
(7) Biesiadka, J.; Loll, B.; Kern, J.; Irrgang, K.-D.; Zouni, A. *Phys. Chem. Chem. Phys.* **2004**, *6*, 4733−4736.
(8) Loll, B.; Kern, J.; Saenger, W.; Zouni, A.; Biesiadka, J. *Nature (London)* **2005**, *438*, 1040−1044.
(9) Pecoraro, V. L.; Baldwin, M. J.; Caudle, M. T.; Hsieh, W.-Y.; Law, N. A. *Pure Appl. Chem.* **1998**, *70*, 925−929.
(10) Tommos, C.; Hoganson, C. W.; Valentin, M. D.; Lydakis-Simantiris, N.; Dorlet, P.; Westphal, K.; Chu, H.-A.; McCracken, J.; Babcock, G. T. *Curr. Opin. Chem. Biol.* **1998**, *2*, 244−252.
(11) Hillier, W.; Wydrzynski, T. *Biochim. Biophys. Acta* **2001**, *1503*, 197−209.
(12) McEvoy, J. P.; Brudvig, G. W. *Phys. Chem. Chem. Phys.* **2004**, *6*, 4754−4763.
(13) McEvoy, J. P.; Gascon, J. A.; Batista, V. S.; Brudvig, G. W. *Photochem. Photobiol. Sci.* **2005**, *4*, 940−949.

10.1021/ic061968k CCC: $37.00
Published on Web 02/13/2007

on the substrate binding by isotope exchange experiments between bulk water and evolved oxygen in PSII preparations[23−28] as well as from studies of proton release from the OEC during the S-state cycle.[29] However, even mechanisms proposed after the availability of the recent PSII crystal structures disagree on the mode of water binding to the OEC; some authors favor terminal water binding,[12−14] and others invoke conversion of the substrate water into a μ-O bridge.[20−22] For the μ-O bridges in the OEC to act as binding sites for substrate waters, water must be able to form a μ-O bridge on a time scale faster than or equal to the time scale of OEC turnover. Measure of the latter time scale has been provided by the isotope exchange experiments on the OEC referred to above.[23−28]

To determine the time scale of μ-oxo exchange, we have recently reported the rates of isotope exchange between μ-O bridges and ^{18}O-labeled water in a series of di-μ-O dimanganese complexes as structural models for the OEC.[30] For the di-μ-O dimers investigated, we observed complete exchange in ∼10−100 min, in line with earlier data.[31] These data provide constraints for the possible involvement of μ-O bridges as water-binding sites in the water oxidation cycle. However, to extend insights gained from the model compounds to the OEC, it is important to have a detailed understanding of the mechanism of exchange in order to better judge how the protein environment of the OEC may affect exchange rates. Here, we report an investigation of the mechanism of oxo exchange between water and the μ-O bridges in di-μ-O di-Mn compounds with and without water-binding sites.

Experimental Section

Materials. The ligand mes−terpy (4′-mesityl-2,2′:6′,2″-terpyridine) and the complexes $[(mes-terpy)_2Mn_2^{III/IV}(\mu\text{-}O)_2(H_2O)_2](NO_3)_3$ (**1**) and $[(phen)_4Mn_2^{III/IV}(\mu\text{-}O)_2](ClO_4)_3$ (**2**), where phen = 1,10-phenanthroline, were prepared according to literature procedures.[32,33] All reagents were used as received. The ligand phen and tetrabutylammonium nitrate were purchased from Sigma Aldrich. Tetrabutylammonium perchlorate was obtained from Acros. Concentrated nitric and perchloric acids were purchased from J. T. Baker. Acetonitrile (HPLC grade) was purchased from Fisher Scientific. $H_2{}^{18}O$ (95 atom % ^{18}O) and $D_2{}^{18}O$ (95 atom % ^{18}O, 99 atom % D) were purchased from Icon Stable Isotopes. ***Safety note:*** *While we have not experienced any problems, perchlorate compounds are potentially explosive and should be handled with appropriate care.*

Isotope Exchange Reactions. Isotope exchange was initiated by adding small volumes of $H_2{}^{18}O$ (95 atom %) into acetonitrile solutions of the compounds **1** or **2**. The use of a nonaqueous solvent was necessary to be able to vary the concentration of water significantly and to attain a high ^{18}O:^{16}O ratio in the water present in the reaction medium (estimated to be up to ∼90 atom % in our experiments) so that large shifts in the ESI-MS isotope patterns could be obtained. After the mixing of the solutions with $H_2{}^{18}O$, the solutions were loaded into a syringe feeding into the mass spectrometer by means of a syringe pump. The time of mixing of $H_2{}^{18}O$ with the solution of **1** or **2** was set as the zero time of exchange. For this reason, $H_2{}^{18}O$ was always the last reagent to be added. For example, in experiments to investigate the effect of free chelating ligand (vide infra), solutions of free mes−terpy or phen were added to solutions of **1** or **2**, respectively, and $H_2{}^{18}O$ was added as the last step before loading the samples into the mass spectrometer.

Experiments to probe the temperature dependence of exchange in **1** were carried out at 20 (ambient temperature), 0, and −13 °C. In the latter two cases, vials containing solutions of **1** were kept in semifrozen water and brine, respectively. After the mixing of **1** with $H_2{}^{18}O$ in the containers, the solutions of **1** were quickly loaded into syringes for injection into the mass spectrometer. The change in temperature during transfer causes ambiguity in the absolute extent of reaction, but the reaction progress between successive measurements is reliable.[30]

ESI-MS. ESI-MS data were collected on a Waters/Micromass ZQ 4000 mass spectrometer and processed with the Masslynx (V 4.0) software and the isotope distribution calculator program at http://www2.sisweb.com/mstools/isotope.htm. Details of the design of the ESI-MS experiments, assignment of peaks, and data analysis have been described previously.[30]

UV−Vis Spectroscopy. UV−vis spectra were recorded on a Varian Cary 50 UV−vis spectrophotometer at room temperature using a 1 cm path length cuvette.

Data Analysis. Monitoring the changes in the isotope patterns for **1** and **2** allowed us to extract the concentrations of unexchanged (U), singly exchanged (S), and doubly exchanged (D) isotopomers as functions of time,[30] and the traces for U were found to fit well to a single-exponential decay of the form $y = A + Be^{-kx}$. Extracting the parameters B and k from the fit enabled us to calculate the initial rates of exchange, given by $-Bk$. This is true even in the case of **1**, where exchange was too fast to obtain data by our experimental method for the initial linear phase of exchange.[30] The initial rate data thus obtained as well as the entire time courses of concentrations of U, S, and D were modeled with the help of the DYNAFIT software,[34] version 3.28.038, available free of charge for academic users from http://www.biokin.com/dynafit.

(14) Isobe, H.; Shoji, M.; Koizumi, K.; Kitagawa, Y.; Yamanaka, S.; Kuramitsu, S.; Yamaguchi, K. *Polyhedron* **2005**, *24*, 2767−2777.
(15) Brudvig, G. W.; Crabtree, R. H. *Proc. Natl. Acad. Sci. U.S.A.* **1986**, *83*, 4586−4588.
(16) Vincent, J. B.; Christou, G. *Inorg. Chim. Acta* **1987**, *136*, L41−43.
(17) Pecoraro, V. L.; Baldwin, M. J.; Gelasco, A. *Chem. Rev.* **1994**, *94*, 807−826.
(18) Yachandra, V. K.; Sauer, K.; Klein, M. P. *Chem. Rev.* **1996**, *96*, 2927−2950.
(19) Nugent, J. H. A.; Rich, A. M.; Evans, M. C. W. *Biochim. Biophys. Acta* **2001**, *1503*, 138−146.
(20) Messinger, J. *Phys. Chem. Chem. Phys.* **2004**, *6*, 4764−4771.
(21) Dasgupta, J.; van Willigen, R. T.; Dismukes, G. C. *Phys. Chem. Chem. Phys.* **2004**, *6*, 4793−4802.
(22) Siegbahn, P. E. M.; Lundberg, M. *Photochem. Photobiol. Sci.* **2005**, *4*, 1035−1043.
(23) Messinger, J.; Badger, M.; Wydrzynski, T. *Proc. Natl. Acad. Sci. U.S.A.* **1995**, *92*, 3209−3213.
(24) Hillier, W.; Messinger, J.; Wydrzynski, T. *Biochemistry* **1998**, *37*, 16908−16914.
(25) Hillier, W.; Wydrzynski, T. *Biochemistry* **2000**, *39*, 4399−4405.
(26) Hendry, G.; Wydrzynski, T. *Biochemistry* **2002**, *41*, 13328−13334.
(27) Hendry, G.; Wydrzynski, T. *Biochemistry* **2003**, *42*, 6209−6217.
(28) Hillier, W.; Wydrzynski, T. *Phys. Chem. Chem. Phys.* **2004**, *6*, 4882−4889.
(29) Junge, W.; Haumann, M.; Ahlbrink, R.; Mulkidjanian, A.; Clausen, J. *Phil. Trans. R. Soc. London, Ser. B* **2002**, *357*, 1407−1418.
(30) Tagore, R.; Chen, H.; Crabtree, R. H.; Brudvig, G. W. *J. Am. Chem. Soc.* **2006**, *128*, 9457−9465.
(31) Larsen, A. S.; Wang, K.; Lockwood, M. A.; Rice, G. L.; Won, T.-J.; Lovell, S.; Sadilek, M.; Tureek, F.; Mayer, J. M. *J. Am. Chem. Soc.* **2002**, *124*, 10112−10123.
(32) Chen, H.; Tagore, R.; Das, S.; Incarvito, C. D.; Faller, J. W.; Crabtree, R. H.; Brudvig, G. W. *Inorg. Chem.* **2005**, *44*, 7661−7670.
(33) Manchanda, R.; Brudvig, G. W.; Gala, S. d.; Crabtree, R. H. *Inorg. Chem.* **1994**, *33*, 5157−5160.

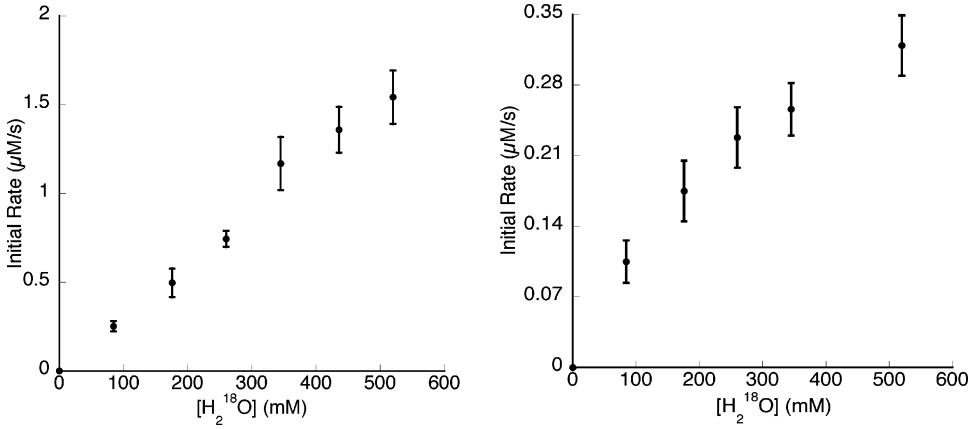

Figure 1. Dependence of initial rates of μ-O exchange on [$H_2{}^{18}O$]. Error bars indicate 1 standard deviation from an average of three or more runs. Left panel: 300 μM **1**. Right panel: 600 μM **2**.

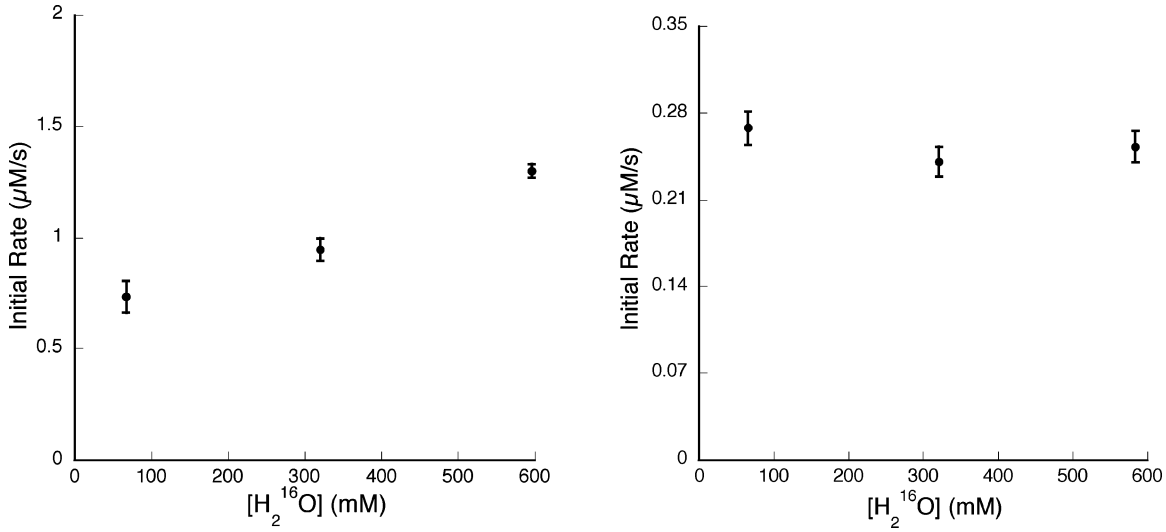

Figure 2. Dependence of initial rates of μ-O exchange on [$H_2{}^{16}O$]. Error bars indicate 1 standard deviation from an average of three or more runs. [$H_2{}^{18}O$] = 260 mM. Left panel: 300 μM **1**. Right panel: 600 μM **2**.

Results

[$H_2{}^{18}O$] Dependence. The dependence of initial rates of μ-O exchange on [$H_2{}^{18}O$] is shown in Figure 1. Compound **1** shows a nearly linear dependence in the concentration range examined (left panel), whereas compound **2** shows a nonlinear saturation behavior in the same concentration range (right panel). Thus, for both complexes, water participates in at least one step that affects the overall rate of exchange.

[$H_2{}^{16}O$] Dependence. If the only role of water in the μ-O exchange process were to supply the isotope label, then increasing [$H_2{}^{16}O$], while keeping [$H_2{}^{18}O$] constant, should either decrease the rate of exchange or leave it unaffected. However, the observed dependence turned out to be different (Figure 2). The rate of exchange for **1** actually increases with increasing [$H_2{}^{16}O$] (left panel), whereas the rate of exchange for **2** remains the same within our experimental error (right panel). The reasons for this behavior are not obvious and need to be addressed by any proposed exchange mechanisms.

Acid Dependence. Addition of small amounts of acids (HNO_3 and $HClO_4$ for **1** and **2**, respectively) to the acetonitrile solutions of **1** and **2** affected the rates of μ-O exchange considerably (Figure 3). During the same time period, there was no evidence of decomposition of the complexes from ESI-MS and UV−vis spectroscopy. Significantly, the direction of the effect of added acid was opposite for **1** and **2**. Whereas exchange rates increased for **1** with the addition of HNO_3 (left panel), they decreased with the addition of $HClO_4$ into solutions of **2** (right panel), indicating that the mechanisms of exchange in **1** and **2** are different. The lack of effect of added (t-Bu_4N)(NO_3) (tetrabutylammonium nitrate) and (t-Bu_4N)(ClO_4) (tetrabutylammonium perchlorate) to **1** and **2**, respectively (vide infra), shows that the effects of HNO_3 and $HClO_4$ are due to protons.

Ionic Strength. The effect of ionic strength on μ-O exchange was investigated by comparison of exchange rates for solutions of **1** and **2** with and without tetrabutylammonium nitrate or tetrabutylammoium perchlorate, respectively. For both **1** and **2**, exchange rates with and without added ions were found to be identical within our experimental error (Supporting Information).

Dependence on Free Ligand. When μ-O exchange of **1** was initiated in the presence of free mes−terpy ligand, the exchange rate was found to be same, within experimental error, of the exchange rate in the absence of free ligand

(34) Kuzmic, P. *Anal. Biochem.* **1996**, *237*, 260−273.

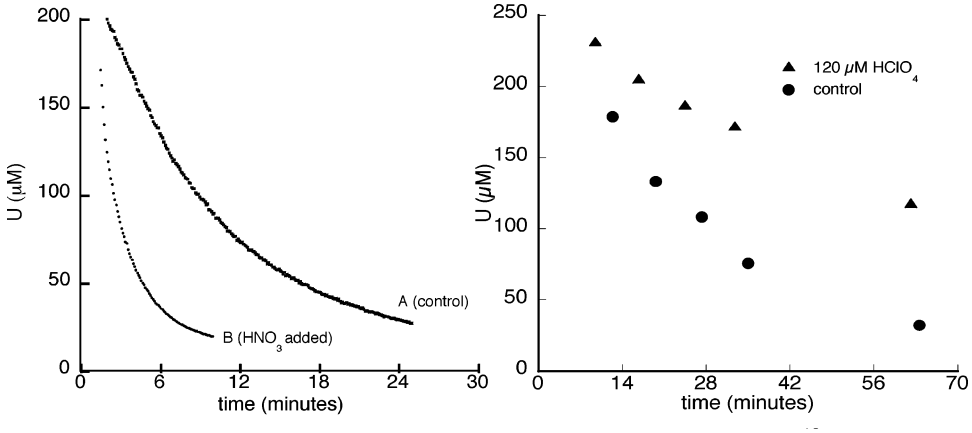

Figure 3. The effect of acid on μ-O exchange rates. (Left panel) 157 mM $H_2{}^{18}O$ added to a solution of 300 μM **1**, with (trace B) and without (trace A) 120 μM HNO_3. (Right panel) 520 mM $H_2{}^{18}O$ added to a solution of 600 μM **2**, with (▲) and without (●) 120 μM $HClO_4$.

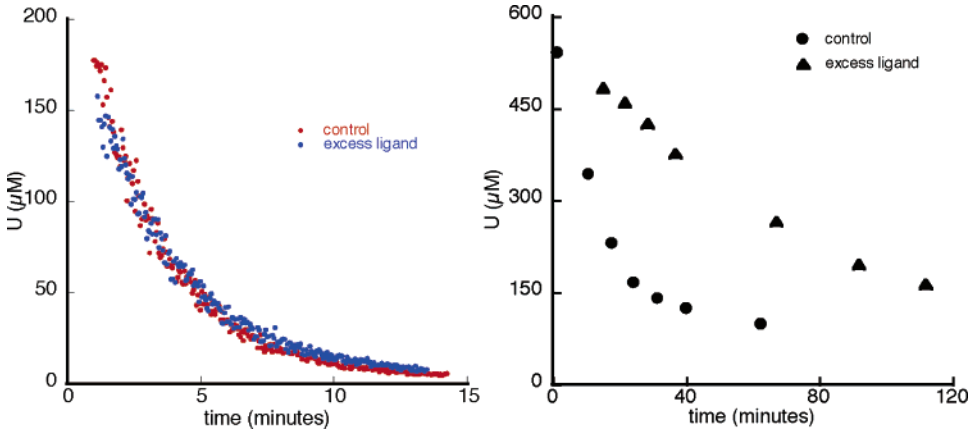

Figure 4. The effect of free ligand on μ-O exchange rates. (Left panel) 520 mM $H_2{}^{18}O$ added to a solution of 600 μM **1**, with (●, in blue) and without (●, in red) 2.4 mM mes−terpy. (Right panel) 520 mM $H_2{}^{18}O$ added to a solution of 600 μM **2**, with (▲) and without (●) 3.6 mM phen.

(Figure 4, left panel). In contrast, the exchange rate for **2** was slower in the presence of free phen ligand as compared with that in the absence of free phen (Figure 4, right panel). This is another indication of different exchange mechanisms for **1** and **2**; the rate or extent of phen ligand dissociation likely contributes to the rate of μ-O exchange in **2**, whereas the dissociation of mes−terpy ligand, if at all required for μ-O exchange in **1**, does not contribute to the exchange rate.

Temperature Dependence of Exchange Rates of 1. An Eyring plot of exchange rates in **1** as a function of temperature is shown in Figure 5. To obtain both the enthalpy and entropy of activation from the Eyring plot, a second-order rate constant must be extracted from measured rates.[35] In the case of **1**, the reaction rate was found to be first order in both [**1**] (Supporting Information) and [$H_2{}^{18}O$] (vide supra), so that a meaningful second-order rate constant, k, could be obtained by dividing the initial rates by the initial [**1**] and [$H_2{}^{18}O$]. The second-order rate constant was divided by the temperature (K), and the natural logarithm of the quotient was plotted as a function of the inverse of the temperature (K) to get a linear plot. The slope of the plot = $-\Delta H^{\ddagger}/R$, and the intercept = $\ln(k_bT/h) + \Delta S^{\ddagger}/R$ ($\Delta H^{\ddagger}$ = enthalpy of activation, $\Delta S^{\ddagger}$ = entropy of activation, R = universal gas constant, T = temperature, k_b = Boltzmann's constant, h = Planck's constant). The values for the slope and intercept, as indicated on the plot, yield the following activation parameters: $\Delta H^{\ddagger} = 9.2 \pm 0.6$ kcal mol^{-1}, $\Delta S^{\ddagger} = -36 \pm 2$ cal mol^{-1} K^{-1}, $\Delta G^{\ddagger} = 20 \pm 1$ kcal mol^{-1} at 300 K ($\Delta G^{\ddagger}$ = Gibbs free energy of activation).

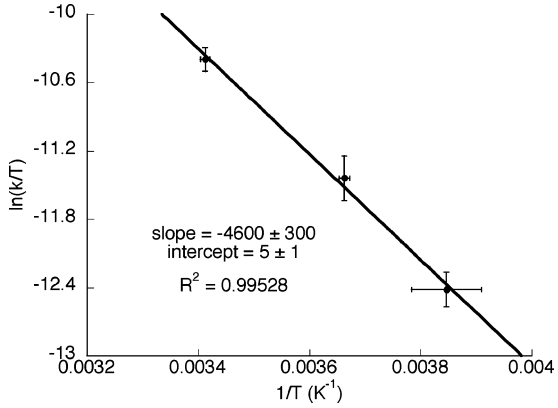

Figure 5. Temperature dependence of μ-O exchange rate in **1**. The linear fit parameters of the Eyring plot are indicated on the plot. Errors on the y-axis indicate 1 standard deviation from the average of three measurements. Errors on the x-axis indicate the range of temperature variation during the experiments.

H/D Isotope Effect on 1. H/D isotope effects on μ-O exchange were investigated for **1**. This was done by comparing exchange rates in the presence of $H_2{}^{18}O$ to those

(35) Lente, G.; Fábián, I.; Poë, A. J. *New J. Chem.* **2005**, *29*, 759−760.

in the presence of $D_2{}^{18}O$. The rates were found to be identical within experimental error (Supporting Information).

Effect of Concentrations of 1 and 2 on μ-O Exchange Rates. We find a first-order dependence of the μ-O exchange rates in **1** and **2** on the concentrations of **1** and **2**, respectively (Supporting Information). Thus, a double-logarithmic plot of initial rates as a function of initial dimer concentration gives a linear plot. Equivalently, plots of the time course of the exchange progress as a percentage of dimer concentration give traces that are independent of dimer concentration. This allows us to rule out rate-determining bimolecular reactions between molecules of (or molecules derived from) **1** and **2**.

Discussion

Choice of Compounds. Compound **1** is closely analogous to $[(terpy)_2Mn_2^{III/IV}(\mu\text{-}O)_2(H_2O)_2](NO_3)_3$ (terpy = 2,2′:6′,2″-terpyridine) (**3**), which has been proposed to be a structural and functional model of the OEC.[36] The presence of the water-binding sites on manganese was identified to be a key feature in achieving catalytic activity, since **3** and analogous $Mn_2(\mu\text{-}O)_2$ dimers with available coordination sites on manganese were found to be active, whereas **2** and analogous coordinatively saturated $Mn_2(\mu\text{-}O)_2$ dimers were found to be inactive.[37] Moreover, the μ-O exchange rates of complexes with and without water-binding sites were found to be significantly different.[30] Bound water, therefore, causes significant differences in reactivity. While several organic-soluble $Mn_2(\mu\text{-}O)_2$ dimers are known in the literature, **1** is one of two known $Mn_2(\mu\text{-}O)_2$ dimers with bound waters that are soluble in nonaqueous solvents.[32] Therefore, we chose **1** and **2** to investigate the effect of water coordination sites on the mechanism of μ-O exchange.

Steps in the μ-Oxo Exchange Process. Isotope exchange between water and bridging oxygens of **1** and **2** must minimally consist of the following steps: (1) Two protonations of the bridging oxygen must occur for it to convert to a free water molecule. (2) Two deprotonations of the labeled water molecule must occur for it to convert to the bridging oxygen atom. (3) The breaking of two bonds between the bridging oxygen and the two manganese atoms being bridged must happen. (4) The formation of two bonds between the oxygen of labeled water and the two manganese atoms to be bridged must take place. An examination of these elementary steps is required to construct a mechanism for bridging-oxo exchange.

Protonation of Oxo Bridges and Deprotonation of Water. Electrochemical studies suggest that whereas the oxo bridges of **2** and the analogous complex $[(bpy)_4Mn_2^{III/IV}(\mu\text{-}O)_2](ClO_4)_3$ (**4**, bpy = 2,2′-bipyridine) remain unprotonated in both aqueous and acetonitrile soution, they can undergo reversible protonations.[38−40] The pK_a's of the μ-O bridges in **2** and **4** have been estimated as ∼2.3 in aqueous solution.[38,39] This suggests a pK_a of ∼9.8 ± 1 in acetonitrile,[41] supported by electrochemical experiments.[40] This value is similar to the values reported for a series of $Mn_2(\mu\text{-}O)_2$ complexes in acetonitrile.[42] Chen et al. have assigned a value of ∼2.5 for the pK_a of the μ-O bridges of **3** in aqueous solution,[43] which is very close to the value for **2** and **4**. The similarity of pK_a values for **2**, **3**, and **4** suggests that the pK_a of **1** will also be similar. Any given acid would, therefore, be expected to protonate the μ-O bridges of **1** and **2** to similar extents.

The only protic hydrogens available in our isotope exchange solutions in the absence of added acids are those from water. Whereas free water has a pK_a of ∼14 and is, therefore, too weak an acid to protonate the μ-O bridges of **1** or **2**, waters coordinated to high-valent manganese centers have a much lower pK_a.[44,45] Unpublished results in our laboratory suggest that the pK_a of water bound to Mn^{IV} in **3** has a pK_a of ∼4.[46]

On the basis of the above values of pK_a's for **2**, **3**, and **4**, we assume pK_a's of ∼2.4 and ∼4 for the μ-O bridge and terminal water, respectively, in **1**. The relative pK_a values are such that the μ-O form would be the major form in solution and yet would provide significant concentrations of the μ-OH form that we propose is required for μ-O exchange (vide infra).

The pK_a considerations discussed above indicate the thermodynamic feasibility of protonating μ-O bridges. Another important consideration is the rate of the protonation process. Rates of thermodynamically favorable protonations of oxygen are often diffusion controlled. However, in the case of μ-O bridges between metal centers, protonation rates could be relatively slow.[47] Reported cases of slow thermodynamically favorable proton transfers[47,48] seem fast enough to not be rate-limiting for μ-O exchange for **1**, **2**, and other oxo-bridged manganese compounds studied previously.[30] However, proton transfer from a terminal water to an oxo bridge in **1** and **2** would be energetically uphill, so the possibility of this step being rate-determining needs to be considered. The absence of an H/D isotope effect in the exchange rate for **1** argues against proton transfer being rate-determining. Since the energetics of the proton transfer are expected to be similar for **1** and **2** on the basis of arguments presented above, we do not expect it to be rate-determining for **1** or **2**.

Opening and Formation of Oxo Bridges. Whereas the rates and extents of protonation of oxo bridges in manganese

(36) Limburg, J.; Vrettos, J. S.; Liable-Sands, L. M.; Rheingold, A. L.; Crabtree, R. H.; Brudvig, G. W. *Science* **1999**, *283*, 1524−1527.
(37) Limburg, J.; Brudvig, G. W.; Crabtree, R. H. *J. Am. Chem. Soc.* **1997**, *119*, 2761−2762.
(38) Cooper, S. R.; Calvin, M. *J. Am. Chem. Soc.* **1977**, *99*, 6623−6630.
(39) Thorp, H. H.; Sarneski, J. E.; Brudvig, G. W.; Crabtree, R. H. *J. Am. Chem. Soc.* **1989**, *111*, 9249−9250.
(40) Manchanda, R.; Thorp, H. H.; Brudvig, G. W.; Crabtree, R. H. *Inorg. Chem.* **1992**, *31*, 4040−4041.
(41) Kristjánsdóttir, S. S.; Norton, J. R. In *Transition Metal Hydrides*; Dedieu, A., Ed.; VCH Publishers: New York, 1992; pp 309−359.
(42) Baldwin, M. J.; Gelasco, A.; Pecoraro, V. L. *Photosynth. Res.* **1993**, *38*, 303−308.
(43) Chen, H.; Faller, J. W.; Crabtree, R. H.; Brudvig, G. W. *J. Am. Chem. Soc.* **2004**, *126*, 7345−7349.
(44) Macartney, D. H.; Sutin, N. *Inorg. Chem.* **1985**, *24*, 3403−3409.
(45) Li, J.; Fisher, C. L.; Chen, J. L.; Bashford, D.; Noodleman, L. *Inorg. Chem.* **1996**, *35*, 4694−4702.
(46) Cady, C.; Crabtree, R. H.; Brudvig, G. W. Manuscript in preparation.
(47) Kramarz, K. W.; Norton, J. R. *Prog. Inorg. Chem.* **1994**, *42*, 1−65.
(48) Carroll, J. M.; Norton, J. R. *J. Am. Chem. Soc.* **1992**, *114*, 8744−8745.

complexes have been measured (vide supra), such data are not available on the opening and closing of these bridges. Protonation of the bridges in μ-O-bridged manganese dimers is known to initiate bridge opening, leading to the formation of monomeric, trimeric, and tetrameric manganese compounds.[39,43,49,50] Examples of formation of oxo bridges between manganese can be found in the synthesis of μ-O-bridged dimers from monomeric precursors.[32] However, in both cases, the rates of the elementary bridge-opening and bridge-formation steps are unknown. A molecular mechanism for μ-O exchange in the hypothetical complex $[(H_2O)_2(OH)_2\text{-}Mn^{IV}(\mu\text{-}O)_2Mn^{IV}(OH)_2(H_2O)_2]$ (**1′**) proposed on the basis of DFT calculations[51] provides benchmark values for the rates of these steps. The activation energies of bridge opening and bridge formation calculated in this theoretical study indicate that bridge opening is much slower than bridge closing. This seems reasonable if bridged species are to retain their bridged structures and is supported by experiments on the interconversion between mono-μ-OH and di-μ-OH Cr(III) dimers.[52]

Previous Studies of Bridging-Oxo Exchange Mechanisms. Data on bridging-oxo exchange rates on Fe,[53,54] Mo,[55,56] Cr,[52,57] Al,[58−63] Rh,[64] and Ru[65] centers have been investigated. The mechanisms of some of these processes have been investigated as well.

Crimp et al. have proposed a mechanism for the exchange of bridging-OH ligands on $Cr_2^{III}(\mu\text{-}OH)_2$ dimers.[57] The proposed mechanism involves the rate-determining opening of the hydroxo bridge, followed by a 180° rotation around the remaining Cr-(μ-OH) bond to switch bridging and terminal positions. An analogous rotation mechanism has been considered for **1′** by Lundberg et al.[51] in their DFT calculations.

Thompson et al. have suggested two mechanisms for exchange between terminal and bridging oxos in a singly bridged $[Mo_2^{V}O_3]^{4+}$ complex.[56] The authors favor the mechanism whereby the oxo bridge bends to bring the metal centers closer together, enabling a terminal oxo to become bridging. The resulting doubly bridged dimer then undergoes a reverse bridge-opening step, such that the originally bridging atom dissociates to become a terminal oxo. The alternate mechanism, which the authors disfavor, involves the dissociation of the dimer into monomers, followed by re-formation of the dimer.

Scheme 1. Proposed Dissociative Mechanism of μ-O Exchange in **1**, Involving Sequential Oxo-Bridge Opening and Labeled Water Coordination

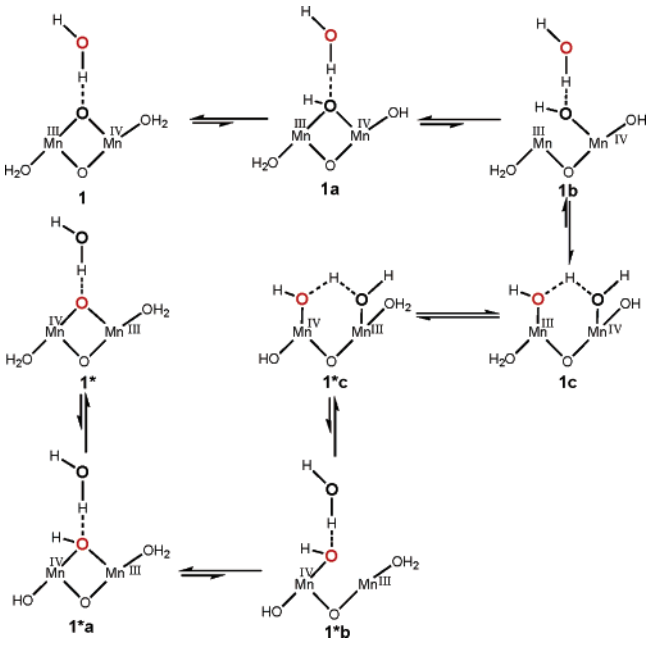

In proposals of mechanisms of μ-OH exchange on aluminum sites, opening of the μ-OH bridge is assigned as rate-determining.[58,60,61] In another case, the opening of a μ_4-O adjacent to the exchanging μ-OH is proposed as rate-determining.[63] The rate-determining bridge-opening step has been proposed as either associative[58] or dissociative.[63] Protonation of the bridge has been proposed to occur before[60,61] or after[58,63] opening. In some cases, intramolecular proton transfer to the bridge is proposed to occur from a coordinated water.[60,61]

In all cases of exchange studies mentioned above, the identity of ligands trans to the exchanging site is seen to be very important in determining rates. For example, exchanging groups trans to hydroxo ligands are found to exchange much faster than ones trans to water.

Mechanism of Exchange in 1. Proposed mechanisms for μ-O exchange in **1** are shown in Schemes 1 and 2, where the red oxygen atoms stand for the isotope labels and asterisks indicate isotopomers. We refer to Schemes 1 and 2 as "dissociative" and "associative", respectively, to indicate oxo-bridge opening without (Scheme 1) and with (Scheme 2) simultaneous formation of the Mn−^{18}O bond. In the following discussion, Scheme 2 is shown to be consistent with our experimental results and with literature results relevant to bridging-oxo exchange pathways. The initial step in the μ-O exchange of **1** is proposed to be a fast protonation

(49) Sarneski, J. E.; Thorp, H. H.; Brudvig, G. W.; Crabtree, R. H.; Schulte, G. K. *J. Am. Chem. Soc.* **1990**, *112*, 7255−7260.
(50) Manchanda, R.; Brudvig, G. W.; Crabtree, R. H. *New J. Chem.* **1994**, *18*, 561−568.
(51) Lundberg, M.; Blomberg, M. R. A.; Siegbahn, P. E. M. *Theor. Chem. Acc.* **2003**, *110*, 130−143.
(52) Spiccia, L.; Marty, W. *Polyhedron* **1991**, *10*, 619−628.
(53) Wilkins, R. G.; Yelin, R. E. *Inorg. Chem.* **1969**, *8*, 1470−1473.
(54) Fleischer, E. B.; Palmer, J. M.; Srivastava, T. S.; Chatterjee, A. *J. Am. Chem. Soc.* **1971**, *93*, 3162−3167.
(55) Richens, D. T.; Helm, L.; Pittet, P. A.; Merbach, A. E.; Nicolo, F.; Chapuis, G. *Inorg. Chem.* **1989**, *28*, 1394−1402.
(56) Thompson, R. L.; Lee, S.; Geib, S. J.; Cooper, N. J. *Inorg. Chem.* **1993**, *32*, 6067−6075.
(57) Crimp, S. J.; Spiccia, L.; Krouse, H. R.; Swaddle, T. W. *Inorg. Chem.* **1994**, *33*, 465−470.
(58) Casey, W. H.; Phillips, B. L.; Karlsson, M.; Nordin, S.; Nordin, J. P.; Sullivan, D. J.; Neugebauer-Crawford, S. *Geochim. Cosmochim. Acta* **2000**, *64*, 2951−2964.
(59) Phillips, B. L.; Casey, W. H.; Karlsson, M. *Nature (London)* **2000**, *404*, 379−382.
(60) Casey, W. H.; Phillips, B. L. *Geochim. Cosmochim. Acta* **2001**, *65*, 705−714.
(61) Lee, A. P.; Phillips, B. L.; Casey, W. H. *Geochim. Cosmochim. Acta* **2002**, *66*, 577−587.
(62) Phillips, B. L.; Lee, A.; Casey, W. H. *Geochim. Cosmochim. Acta* **2003**, *67*, 2725−2733.
(63) Rustad, J. R.; Loring, J. S.; Casey, W. H. *Geochim. Cosmochim. Acta* **2004**, *68*, 3011−3017.
(64) Drljaca, A.; Zahl, A.; van Eldik, R. *Inorg. Chem.* **1998**, *37*, 3948−3953.
(65) Hurst, J. K.; Zhou, J.; Lei, Y. *Inorg. Chem.* **1992**, *31*, 1010−1017.

Scheme 2. Proposed Associative Mechanism of μ-O Exchange in **1**, Involving Concerted Oxo-Bridge Opening and Labeled Water Coordination

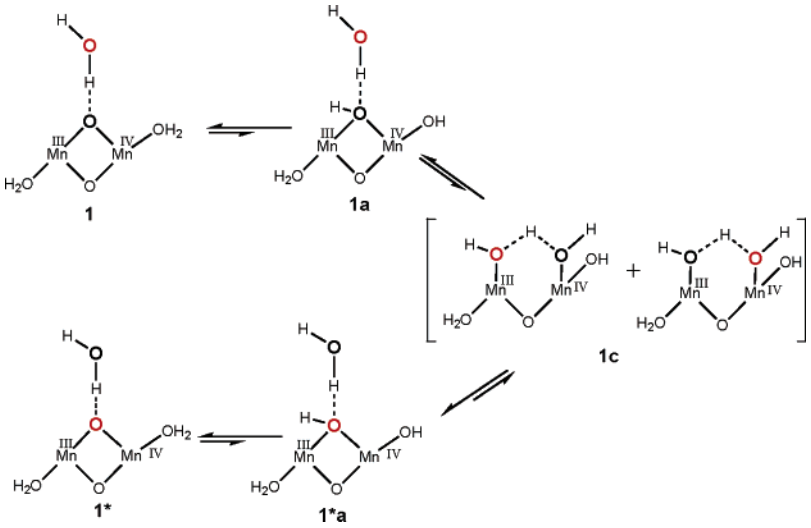

of a μ-O bridge by water coordinated to Mn^{IV}. Bridge opening without initial protonation has been proposed for $Cr_2^{III}(\mu\text{-OH})_2$ dimers[57] as well as for oxo-bridged aluminum clusters.[58,63] However, these examples involve opening of a μ-OH bridge or the conversion of a μ_4-O into a μ-O, whereas in the case of **1**, such a step would produce a strongly basic oxide ion on high-valent manganese. In view of the pK_a of the μ-O of **1**, estimated to be ~2.5,[43] protonation preceding bridge opening would seem to be energetically more favorable. Similar proposals have been made for oxo-exchange in aluminum−oxo clusters.[60,61] Moreover, protonation is known to initiate bridge opening in manganese dimers.[38,39,43,49,50] Protonation from the water coordinated to the Mn^{IV} site is expected, since it is more acidic than bulk water or the water coordinated to the Mn^{III} site. The energetic feasibility of such a protonation has been discussed above. The protonation step is proposed to be fast on the time scale of exchange, as justified by measured rates of protonation of oxo bridges in manganese dimers,[47,48] and the observed absence of H/D isotope effects in our experiments.

Protonation of the bridge is expected to be intramolecular, based on the first-order dependence of the rate of exchange on [**1**]. Such an intramolecular reaction is advantageous, being inherently entropy-favored over an intermolecular reaction. Intramolecular oxo-bridge protonation from coordinated water has been proposed for aluminum−oxo clusters.[60,61]

Protonation of the oxo-bridge is followed by a slow detachment of the protonated bridge and coordination of water at the vacated site. Since the intervalence charge-transfer process is expected to be fast on the time scale of the slow bridge-opening process,[38,66] a distinction between Mn^{III} and Mn^{IV} centers may not be relevant at this stage. Opening of the bridge could precede water coordination (dissociative opening) or could happen concurrently (associative opening). Dissociative opening has been suggested for the μ-OH bridges in $Cr_2^{III}(\mu\text{-OH})_2$ dimers by Crimp et al.[57] and is also favored for **1′** by Lundberg et al.[51] In contrast, our temperature-dependence experiment yields a large negative entropy of activation, favoring an associative RDS. It is conceivable that second shell solvent reorganization could account for a negative entropy of activation in a formally dissociative RDS. The value of −36 cal mol^{-1} K^{-1} measured for $\Delta S^{\ddagger}$ in our experiment corresponds to a contribution of +10.8 kcal mol^{-1} to $\Delta G^{\ddagger}$ at 300 K. To overcome the inherently positive entropy contribution from bond dissociation and create a net $\Delta S^{\ddagger}$ of such magnitude would seem to require an unusually large ordering of H bonds around the TS as compared with the reactant. Moreover, the rather small value of 9.2 kcal mol^{-1} measured for $\Delta H^{\ddagger}$ is consistent with an associative mechanism. Nevertheless, we consider both dissociative and associative mechanisms in the simulation of the μ-O exchange reaction (see below). Whether or not bridge opening is accompanied by water coordination, we assign it to be a slow step. The remaining steps after bridge opening and label coordination are the reverse of the preceding steps, so that the mechanism is symmetric with respect to the identity of the label. To make the dissociative mechanism symmetric, we require the interconversion between species **1c** and **1*c**, which involves intramolecular proton transfer. Both proton (vide supra) and electron transfer[38,66] are expected to be fast on the oxo-exchange time scale.

The activation parameters obtained from the observed temperature dependence of exchange rates, the lack of a H/D kinetic isotope effect, and the lack of effect of added mes−terpy ligand are qualitatively consistent with the proposed exchange mechanisms. The effect of added acid is rationalized by an increase in the protonated form of the dimer, leading to increased exchange rates, whereas the lack of effect of added mes−terpy is reasonable due to the lack of involvement of mes−terpy ligand in the oxo-exchange pathway.

Simulation of Proposed Mechanism for 1. We simulated the observed dependences of exchange rates on $[H_2{}^{18}O]$ and $[H_2{}^{16}O]$ with the help of the DYNAFIT program for the

(66) Cooper, S. R.; Dismukes, G. C.; Klein, M. P.; Calvin, M. *J. Am. Chem. Soc.* **1978**, *100*, 7248−7252.

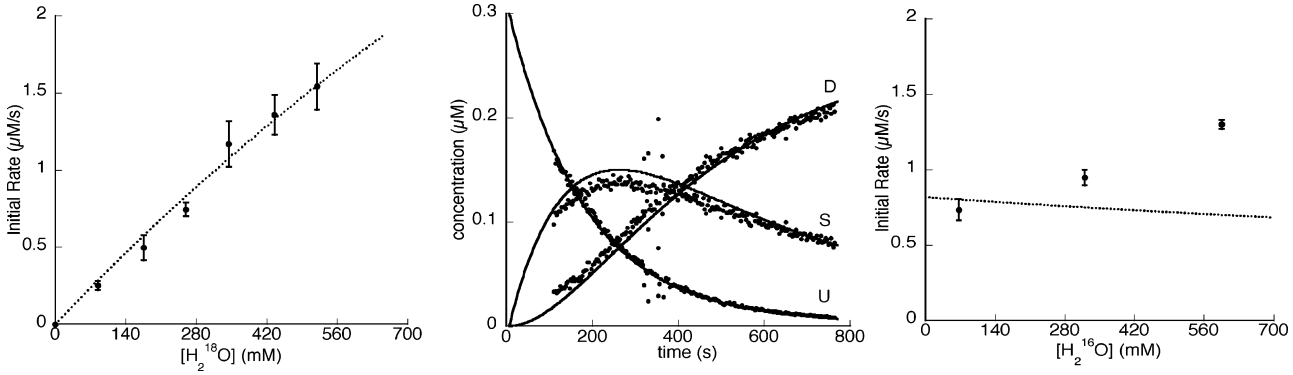

Figure 6. Simulation of exchange data for **1** according to the dissociative pathway indicated in Scheme 1. (Left panel) Initial exchange rates as a function of $[H_2{}^{18}O]$. Experimental data are the same as in the left panel of Figure 1. The dotted line represents the simulated $[H_2{}^{18}O]$ dependence. (Middle panel) Experimental (data points) and simulated (lines) time courses of unexchanged (U), singly exchanged (S), and doubly exchanged (D) forms of **1** for μ-O exchange with [**1**] = 300 μM, $[H_2{}^{18}O]$ = 520 mM. (Right panel) Initial exchange rates as a function of $[H_2{}^{16}O]$, for $[H_2{}^{18}O]$ = 260 mM. Experimental data are the same as in the left panel of Figure 2. The dotted line represents the simulated $[H_2{}^{16}O]$ dependence.

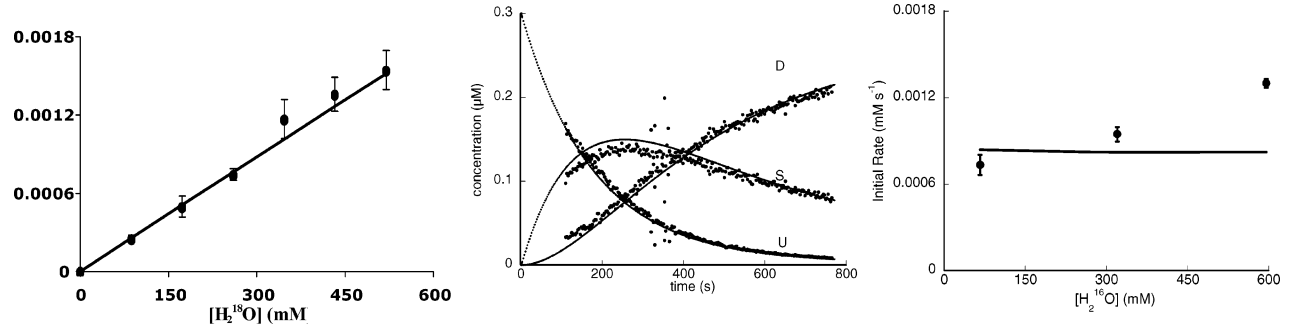

Figure 7. Simulation of exchange data for **1** according to the associative pathway indicated in Scheme 2. (Left panel) Initial exchange rates as a function of $[H_2{}^{18}O]$. Experimental data are the same as in the left panel of Figure 1. The line represents the simulated $[H_2{}^{18}O]$ dependence. (Middle panel) Experimental (data points) and simulated (lines) time courses of unexchanged (U), singly exchanged (S), and doubly exchanged (D) forms of **1** for μ-O exchange with [**1**] = 300 μM, $[H_2{}^{18}O]$ = 520 mM. (Right panel) Initial exchange rates as a function of $[H_2{}^{16}O]$, for $[H_2{}^{18}O]$ = 260 mM. Experimental data are the same as in the left panel of Figure 2. The line represents the simulated $[H_2{}^{16}O]$ dependence.

analysis of reaction kinetics and equilibria.[34] Although we favor an associative mechanism, we simulated concentration dependences for both the dissociative and associative mechanisms. The details of the simulation are given as Supporting Information.

Simulation according to the dissociative mechanism (Scheme 1) reproduces the observed $[H_2{}^{18}O]$ dependence and the time courses of the isotopomers of **1** during exchange (Figure 6, left and middle panels). The water coordination step in this mechanism occurs after the slow bridge-opening step, and as such it may be expected that water concentration would not have an effect on the rate. However, the bridge-opened intermediate in the dissociative mechanism can either undergo bridge closing to go back to the reactant or undergo water coordination to proceed toward exchange. If the bridge-closing reaction were much faster than water coordination, water coordination, though much faster than the bridge-opening step, would become rate-limiting. An attempt to simulate the observed $[H_2{}^{16}O]$ dependence with the same dissociative scheme and rate constants as those used for simulations of $[H_2{}^{18}O]$ dependence and time courses gives a poor fit (Figure 6, right panel).

We then used the associative pathway indicated in Scheme 2 for simulating the experimental exchange data. The results are shown in Figure 7. The dependence of initial exchange rates on $[H_2{}^{18}O]$ and the time course of isotopomers are again successfully simulated (left and middle panels). The simulation of $[H_2{}^{16}O]$ dependence of initial exchange rates, although somewhat better than the simulation for the dissociative scheme, is again poor (right panel).

To rationalize enhancement of exchange rates by unlabeled water, we need to invoke participation of water in a capacity other than the carrier of the oxygen label. If the only role of water in the exchange process is to supply the isotope label, then unlabeled water must necessarily inhibit the exchange or have no effect on it. The absence of any effect can be rationalized, for example, by a mechanism in which the only RDS involves an intramolecular rearrangement of the dimer before it interacts with water. However, in such cases, neither labeled nor unlabeled water will have any effect on the exchange rate. The present case, showing a linear dependence of exchange rate on $[H_2{}^{18}O]$, is clearly different. The observed increase of exchange rates due to unlabeled water must, therefore, be due to a facilitatory role of water that is independent of the identity of its oxygen isotope.

The protic hydrogens of water could facilitate the exchange process by forming H bonds in a manner that lowers the energy of the exchange pathway. Alternatively, varying the amount of unlabeled water could change the dielectric constant of the medium and account for the changes in exchange rates. The lack of effect of ionic strength (see Supporting Information) seems to suggest that the dielectric does not have a big effect on exchange rate. However, the change in dielectric constant due to changes in water

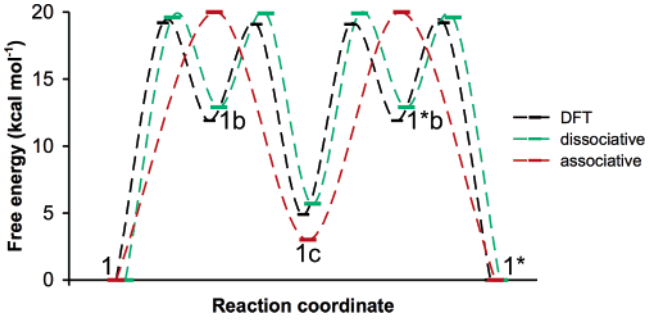

Figure 8. Energy profiles for μ-O exchange in **1**, simulated according to the associative (red) and dissociative (green) pathways shown in Schemes 1 and 2, superimposed on the energy profile for μ-O exchange in **1′** calculated from DFT (black) in ref 51.

concentrations may be much larger than that due to changes in ionic strength, and at present we cannot rule out changes in dielectric constant as the source of the effect of unlabeled water. H bonding to second shell waters and changes in dielectric could exhibit ambiguous nonstoichiometric concentration dependencies, even for elementary steps. We have not attempted to account for such interactions, since that would greatly increase the complexity of the mechanistic scheme. However, as a working hypothesis, we attribute the anomalous dependence of exchange rates on [$H_2{}^{16}O$] to H bonding interactions of second-shell waters.

We note that $H_2{}^{18}O$ and $H_2{}^{16}O$ will be identical with respect to H bonding effects or any other effect not involving the identity of the oxygen isotope. Our simulation, despite leaving out an isotope-independent effect of water, predicts the correct dependence of exchange rates on [$H_2{}^{18}O$]. In other words, the simulation overemphasizes the effect of label content in order to arrive at the correct observed [$H_2{}^{18}O$] dependence. The overemphasis on label content would then lead to the prediction of a more negative dependence on [$H_2{}^{16}O$] as compared with the actual dependence. This is indeed what is observed.

The energy profile diagrams constructed on the basis of simulations of the dissociative and associative pathways indicated in Schemes 1 and 2 are shown in Figure 8. The energy profile calculated by Lundberg et al. on the basis of their DFT calculations on [$(H_2O)_2(OH)_2Mn^{IV}(\mu\text{-}O)_2Mn^{IV}(OH)_2(H_2O)_2$] (**1′**)[51] is shown for comparison. The close match of the energy profile of our dissociative scheme with the DFT energy profile may be fortuitous, since **1′** differs from **1** in the manganese oxidation states and in the ligand set on manganese. The higher oxidation state of **1′** is expected to lead to slower exchange,[30] whereas the presence of hydroxides is expected to lower the positive charge on manganese and labilize the μ-O groups, leading to faster exchange. It is possible that these opposing effects balance out to produce the same exchange rates in **1** and **1′**.

Mechanism of Exchange in 2. Upon a comparison of the kinetic data obtained for μ-O exchange of **1** and **2**, it is clear that they follow different mechanisms of exchange. Whereas somewhat different dependences on labeled and unlabeled water could come about due to different relative magnitudes of rate constants for a sequence of steps in a given mechanism, it is not clear how the same mechanism can explain the opposite effect of added acid on the exchange rates for **1** and **2**. The absence of effect of added mes−terpy on the exchange rate for **1** and the considerable slowing of exchange rate for **2** in the presence of free phen further support the notion that the exchange mechanisms are considerably different between **1** and **2**. On the basis of the dependence on added acid and free phen ligand, we propose the requirement of dissociation of a phen ligand, which is followed by water coordination, as shown in Scheme 3, prior to exchange of the μ-O bridge.

The pyridine rings of the phen ligand are linked rigidly by a −CH=CH− backbone and cannot undergo sequential decoordination. Instead, the coordinating nitrogens of both pyridine rings decoordinate together. The vacated coordination sites thus created would be filled up by water ligands. This results in the formation of **2a**$(\mu\text{-}O)_2(H_2O)_2$ from **2**, as shown in eq 1 of Scheme 3. On the basis of previous studies of ligand decoordination in **2** and **4**, the conversion of **2** to **2a**$(\mu\text{-}O)_2(H_2O)_2$ is proposed to occur on a time scale of about 1 s.[50,67] Considering the ligand set on Mn^{III} in **2a**$(\mu\text{-}O)_2(H_2O)_2$, we suggest a deprotonation of the water trans to the oxo bridge to form the stronger hydroxo ligand. The Jahn−Teller distortion causes the bond to the water trans to the oxo bridge to be shorter than that for the water cis to oxo bridge. The trans water is, therefore, more acidic. The proton could be transferred intramolecularly to an oxo bridge (eq 2) or to a free phen or water molecule (eqs 3 and 4, respectively). In the instance where the proton is transferred to the oxo bridge, the species **2a**$(\mu\text{-}O)(\mu\text{-}OH)(OH)(H_2O)$, containing a μ-OH bridge trans to a hydroxo ligand, is formed. This species, having a labilized protonated bridge, is analogous to **1a** in Scheme 2 and could undergo μ-O exchange by the same pathway. In other words, μ-O exchange in **2** involves the formation of **2a**$(\mu\text{-}O)_2(H_2O)_2$ from **2** as shown in Scheme 3, followed by the conversion of **2a** to **2a*** in the same way as the conversion of **1** to **1*** in Scheme 2.

The requirement for loss of phen for μ-O exchange in **2** provides explanations for (1) the slow rate of μ-O exchange as compared to **1**, (2) inhibition of exchange by added phen ligand, and (3) inhibition of exchange by stoichiometric amounts of acid. The slow rate of exchange is explained by the position of the equilibrium of eq 1, which lies predominantly to the left and thus affords a relatively small concentration of the exchangeable species **2a**$(\mu\text{-}O)_2(H_2O)_2$. Once formed, **2a**$(\mu\text{-}O)_2(H_2O)_2$ prefers to undergo the reverse reaction to re-form **2** instead of proceeding toward μ-O exchange. Addition of phen ligand further shifts the equilibrium to the left, thus slowing exchange (Figure 4, right panel). To explain the effect of added acids, we note that freshly made aqueous solutions of **2** are acidic. This suggests that there is a net release of protons into solution in the process of conversion of **2** to the aqua species **2a**. Addition of stoichiometric quantities of protons would, therefore, shift

(67) Manchanda, R. *Inorganic Models with Relevance to the Oxygen-Evolving Center of Photosystem II*; Yale University: New Haven, CT, 1994.

Scheme 3. Ligand Dissociation and Water Coordination to **2** Proposed as Requirements for μ-O Exchange

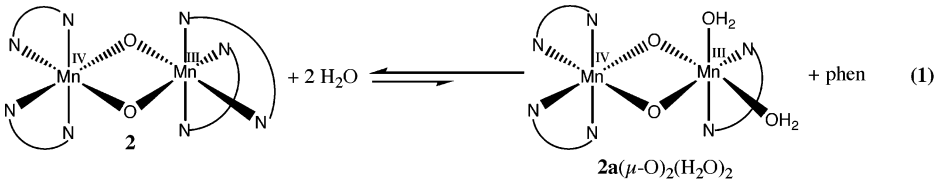

the equilibrium toward **2**, inhibiting the μ-O exchange process (Figure 3, right panel).

We have not simulated the kinetic data for **2**, since there would be a greater number of steps and rate constants as compared with the kinetic schemes for **1**. We feel that a simulation with such a large number of parameters will not be meaningful given the present data.

Isotope Exchange in the OEC. A primary objective of this work was to investigate in detail the mechanism of μ-O exchange in di-μ-O di-Mn model complexes to assess the possibility of the involvement of μ-O bridges in the OEC as substrate-binding sites. Toward this end, we have previously measured the rates of μ-O exchange in a series of di-μ-O di-Mn complexes.[30] The comparison of exchange rates between different model complexes showed that (1) metal centers that remain in a Mn^{IV} oxidation state exchange much slower than those which can switch between Mn^{IV} and Mn^{III} states and (2) the availability of terminal water-binding sites on manganese enhances μ-O exchange rates. These two factors need to be accounted for in a comparison of μ-O exchange rates.

We also compared the absolute rates measured in the model complex **1** to the fast and slow isotope exchange rates measured in PSII samples.[23−28] The S_1 and S_2 oxidation states of the OEC are widely accepted to be $Mn_2^{III}Mn_2^{IV}$ and $Mn^{III}Mn_3^{IV}$, respectively. The exchange rate in the mixed-valent $Mn_2^{III/IV}$ complex **1** was, therefore, considered to be a reasonable model for the exchange rates in the S_1 and S_2 states of the OEC. The fast exchange rates in the S_1 and S_2 states are $\sim 10^5$ times greater than the μ-O exchange rate in **1**. The rate of fast exchange in the OEC is smallest in the S_3 state but is still $\sim 10^3$ times greater than that in **1**. Thus, it is very unlikely that the fast isotope exchange rates measured in the OEC are μ-O exchange rates.

The slow isotope exchange rates measured in the S_0, S_2, and S_3 states are ~800−4000 times greater than those in **1**, and it is, therefore, also very unlikely that the slow isotope exchange rates measured in the S_0, S_2, and S_3 states of the OEC are μ-O exchange rates. The slow exchange rate in the S_1 state of the OEC, however, approaches the μ-O exchange rate for **1**, being ~8 times greater. The activation energy for the slow exchange measured in the S_1 state is ~83 kJ mol^{-1},[28] which is close to the activation energy for μ-O exchange calculated for **1′**[51] (~80 kJ mol^{-1}) and to that observed in this work for **1** (~84 kJ mol^{-1}). Thus, our data are consistent with the slow exchanging substrate in the S_1 state being bound as a bridging oxo.

From the perspective of metal oxidation states, the direct comparison of μ-O exchange rates between **1** and the OEC is reasonable. However, differences in other factors need to be considered to make a rigorous comparison between the μ-O exchange rates in the OEC and **1**. We have identified some of these factors in the course of our investigation of the mechanism of μ-O exchange in **1** and **2**, as discussed below. In addition to the factors discussed below, there are likely to be other subtle factors operating in a protein active site, which may be difficult to investigate by a study of model complexes. As an example, we note that the exchange rate of $\sim 8 \times 10^{-4}$ s^{-1} attributed to μ-O exchange in the Fe−(μ-O)−Fe center of ribonucleotide reductase[68] is $\sim 10^4$ times smaller than the rates of μ-O exchange measured in inorganic Fe−(μ-O)−Fe complexes (~1−40 s^{-1}).[53,54] The possibility of a similar disparity in the comparison of **1** and the OEC should be kept in mind, considering the restricted and rigidly structured nature of the OEC active site, which could inhibit exchange.

Terminal Water-Binding Sites. We have previously shown that the absence of terminal water-binding sites on manganese inhibits μ-O exchange.[30] In the present study, we show that dissociation of chelating ligands is required for μ-O exchange when terminal water-binding sites are not available. Since dissociation of protein residues may be unlikely in the OEC, μ-O exchange may not readily occur unless terminally bound waters are present. Thus, if the slow exchanging substrate in the OEC is bound as a μ-O ligand, the OEC also may need to contain terminal waters to account for exchange rates in the OEC that are greater than the exchange rate in **1**. Alternatively, the slow exchanging substrate could be a terminal water or hydroxo ligand. In either case, the presence of terminally bound water ligands on the OEC is implicated.

pH. We find a considerable effect of proton concentration on μ-O exchange rates in **1** and **2**. The oxygen isotope exchange rates in the OEC referred to above were measured at pH 6, which would correspond to micromolar concentrations of protons in the medium. This is not unlike the proton concentration range used in our acid-dependent experiments, where the acid concentrations varied from ~0 to 120 μM.

(68) Sjoberg, B.-M.; Loehr, T. M.; Sanders-Loehr, J. *Biochemistry* **1982**, *21*, 96−102.

At these concentrations, the exchange rates were affected by factors of ~2−7. Thus, any differences in μ-O exchange rates due to pH between the OEC and **1** are not expected to be very large.

Dielectric Environment. The local dielectric constant in the interior of the OEC is expected to be considerably lower than that of water. Our exchange measurements are done in acetonitrile, which also provides a relatively low dielectric environment compared to water. Additionally, we see that ionic strength of the medium does not affect exchange rates, suggesting that small variations in the dielectric constant of the medium do not affect μ-O exchange rates.

Hydrogen Bonding. Our data suggest that the presence of hydrogen bonds facilitates μ-O exchange. Well-structured hydrogen-bonding networks are likely to be present in the OEC and could enhance μ-O exchange. The observation of an H/D isotope effect has been taken as evidence of influence of H bonding on the exchange rates in the OEC.[28] The fast exchange was seen to have an inverse isotope effect, whereas the slow exchange was seen to remain unaffected. On the basis of the small magnitude of the isotope effect, it was attributed to secondary hydrogen-bonding effects. Similarly, we see small effects attributed to hydrogen bonding to second-shell waters, so the presence of more extensive hydrogen bonding in the OEC is unlikely to enhance μ-O exchange to any great extent as compared to **1**.

Label Concentration. We find a first-order or lower dependence of μ-O exchange rates upon the concentration of labeled water in the concentration range of ~0.1−0.6 M. The label concentration used in the OEC experiments was ~7.4 M; the effective concentration at the site of exchange is likely to be smaller, considering the buried nature of the OEC. Extrapolating the μ-O exchange rate for **1** to a concentration of 7.4 M $H_2{}^{18}O$, assuming first-order dependence, gives a rate of 7.5×10^{-2} s^{-1} that is similar to the slowest exchange rate measured in the OEC (2.2×10^{-2} s^{-1} for the slow exchange rate in the S_1 state) but much smaller than the fast exchange rates in all states and the slow exchange rates in the S_0, S_2, and S_3 states.

Summary and Conclusions

We have investigated the mechanism of μ-O exchange in $Mn_2{}^{III/IV}(\mu\text{-O})_2$ dimers with and without terminal water-binding sites. Our results are consistent with the requirement of bridge protonation prior to the rate-determining opening of the μ-O bridge and concerted coordination of water at the vacated site. For a di-μ-O Mn dimer without terminal water-binding sites, ligand dissociation and water coordination at the vacated site(s) are necessary for μ-O exchange to occur. The data are suggestive of a facilitatory role of hydrogen bonding in the μ-O exchange process.

On the basis of the mechanistic insight gained in this work, we reexamine our previous conclusions regarding the binding mode of substrate waters in the OEC.[30] We reinforce our conclusion that the fast exchanging substrate in the OEC and the slow exchanging substrate in the S_0, S_2, and S_3 states are terminally bound. A μ-O binding mode remains a possibility for the slow exchanging substrate in the S_1 state, with the constraint that the exchange of this substrate involves facilitation by a fully protonated water terminally bound to the OEC.

Acknowledgment. This work has been supported by the National Institutes of Health (GM32715). We are grateful to Dr. Petr Kuzmic for help with the DYNAFIT software.

Supporting Information Available: The effects of dimer concentration and ionic strength on bridging-oxo exchange rates in **1** and **2**, H/D isotope effects on exchange rate in **1**, mechanistic scheme used for the simulation of experimental data for **1**, and the optimized rate constants obtained from the simulation. This material is available free of charge via the Internet at http://pubs.acs.org.

IC061968K